

## Study of Phonon Dispersion in Silicon and Germanium at Long Wavelengths Using Picosecond Ultrasonics

H.-Y. Hao and H. J. Maris

*Department of Physics, Brown University, Providence, Rhode Island 02912*

(Received 10 February 2000)

We have studied the dispersion of long wavelength longitudinal phonons in silicon and germanium using ultrasonic techniques. For long wavelengths, the acoustic phonon dispersion relation is of the form  $\omega(k) \approx ck - \gamma k^3$ , where  $c$  is the speed of sound and  $\gamma$  measures the lowest-order phonon dispersion. By sending an ultrasonic pulse of length a few hundred angstroms into a crystal and measuring the change of the pulse shape with propagation distance, we are able to determine the parameter  $\gamma$ . The results are compared with lattice dynamics models.

PACS numbers: 63.20.-e

The dispersion of phonons in crystals has been studied by a number of methods, including Raman, x-ray, and neutron scattering [1,2]. While these techniques can determine the dispersion relation over the entire Brillouin zone, they have limited accuracy for long wavelength acoustic phonons. These phonons are of special interest because their dispersion is sensitive to the long range part of the interatomic potential [3]. They have been studied, for example, by energy-selective phonon focusing experiments [4,5]. In this Letter we will describe how the picosecond ultrasonics technique [6] can be used to measure the dispersion of longitudinal acoustic phonons.

The propagation of a disturbance along a chain of particles was first discussed qualitatively by Baden-Powell in 1841 [7]. Later Hamilton [8,9] worked on this problem and obtained the exact solution for the motion of a one-dimensional chain of particles each of mass  $M$ , with interparticle spacing  $a$ , and connected by nearest-neighbor springs of strength  $\beta$ . Hamilton considered a situation in which at time zero all atoms were at rest at their equilibrium positions, except for a single particle (the 0th particle) which was given a displacement  $u_0$ . He showed that at time  $t$  the displacement  $u_n(t)$  of the  $n$ th particle in the chain was

$$u_n(t) = u_0 J_{2n}(\omega_0 t), \quad (1)$$

where  $\omega_0 = (4\beta/M)^{1/2}$ . For large  $n$ , the displacement is extremely small until a time  $2n/\omega_0$  has elapsed. This is the time for sound to travel along the chain to the  $n$ th particle; the sound velocity  $c$  is equal to  $(\beta a^2/M)^{1/2}$ . After this time the particle oscillates with an increasing frequency. Figure 1 shows the displacement of the 150th particle along the chain as a function of time.

In the long wavelength limit, acoustic phonons have a linear dispersion relation  $\omega = ck$ . If a pulse disturbance is composed entirely of components having wave number sufficiently small that the approximation  $\omega = ck$  is valid, then the pulse will propagate without any change in shape. The oscillations that are seen in Fig. 1 are a consequence of phonon dispersion; i.e., they result from components of the disturbance for which the phonon frequency  $\omega$  is not

well approximated by  $ck$ . The frequency of the oscillations is determined by the strength of the dispersion and by the distance that the pulse has traveled. As an example, we note that for small  $k$  the dispersion relation can be approximated by the form

$$\omega(k) = ck - \gamma k^3 + \dots, \quad (2)$$

where the coefficient  $\gamma$  will be referred to as the dispersion parameter. Based on this form, it is straightforward to show that the frequency  $\Omega$  of the oscillations that result from dispersion is given by the formula

$$\Omega = c^2 \sqrt{\frac{\gamma}{3\gamma x}}, \quad (3)$$

where  $x$  is the distance that the pulse has traveled, and  $\gamma$  is the time measured from the front of the pulse, i.e.,

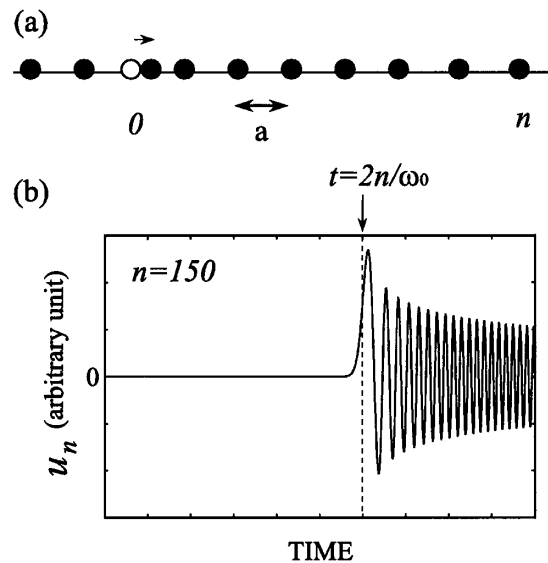


FIG. 1. (a) In a one-dimensional lattice the atom 0 is disturbed at  $t = 0$ . (b) Displacement  $u_{150}$  of the 150th atom as a function of time. The dashed vertical line indicates the arrival time of a disturbance traveling at the speed of sound. The oscillations after the main pulse arise from phonon dispersion.

$\tau \equiv t - x/c$ . This formula holds provided that  $x/c \gg \tau \gg \Omega^{-1}$ . A measurement of the frequency of the oscillations can be used to determine the value of the dispersion parameter  $\gamma$ .

Suppose that a pulse of spatial width  $\Delta x$  is launched into a crystal. This pulse will contain components with wave number of the order of  $1/\Delta x$ . Hence, the different components will have phase velocities that vary by a fraction of the order of  $\gamma/c(\Delta x)^2$ . After the pulse has traveled a total distance  $x$ , dispersion will have broadened the pulse by an amount  $x\gamma/c(\Delta x)^2$ . Thus, in order for dispersion to significantly change the pulse shape, it is necessary that  $x\gamma/c(\Delta x)^2 > \Delta x$ ; i.e., the propagation distance has to exceed

$$x = \frac{c(\Delta x)^3}{\gamma}. \quad (4)$$

For pulses generated in conventional ultrasonic experiments at 5 MHz, for example,  $\Delta x$  is of the order of 0.1 cm. The order of magnitude of  $\gamma$  is  $10^{-11} \text{ cm}^3 \text{ s}^{-1}$ , and so such a pulse would have to travel about  $10^9$  km in order for dispersion to modify the pulse shape. To observe the effect of phonon dispersion, it is necessary to use very short sound pulses. By means of picosecond ultrasonic techniques, it is now possible to generate and detect sound pulses as short as 100 Å. For such pulses, the distance  $x$  can be on the scale of millimeters or even less.

The experimental setup is shown schematically in Fig. 2. The sample is a wafer of Si or Ge with both faces highly polished. An Al film of thickness 240 to 300 Å is deposited on one side of the wafer, and is used as an ultrasonic transducer. An optical pump pulse of duration 200 fs is focused onto an area of the Al film, and abruptly raises the temperature by a few K. This sets up a thermal stress, and a longitudinal acoustic pulse with a spectrum that peaks at a frequency of about 120 GHz is launched into the sample. This acoustic pulse travels across the crystal, and is reflected with a sign change at the far surface.

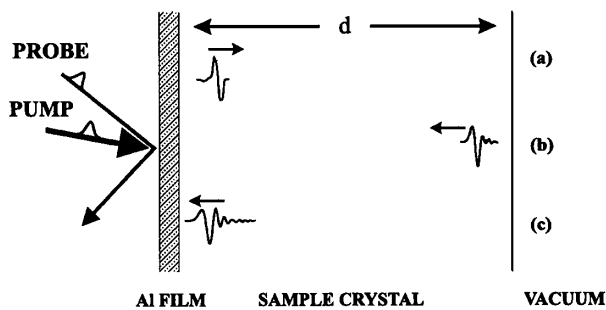


FIG. 2. Schematic diagram of the experiment for studying the phonon dispersion in crystalline solids. (a) A light pulse is absorbed in the Al film and an acoustic pulse is generated. (b) The pulse propagates across the crystal and is reflected at the far surface. (c) The pulse returns to the Al transducer with a shape modified by dispersion, and is then detected by a probe light pulse.

When the pulse reenters the Al transducer film, it causes a small change  $\Delta R$  in the optical reflectivity of the film. By using a time-delayed optical probe pulse to measure  $\Delta R(t)$  as a function of time  $t$ , we can measure the shape of the acoustic echo.

A Ti:sapphire mode-locked laser is employed as the optical source. The wavelength is 800 nm, and the repetition rate is 75.5 MHz (time between pulses of 13.25 ns). Since the change of reflectivity is very small [ $\Delta R(t)/R \sim 10^{-5}$ ], lock-in techniques are used to improve signal to noise. The travel time for the first acoustic echo is usually in the range 100 ns to several  $\mu\text{s}$ , and it would be inconvenient to produce a probe pulse with this delay through the use of a conventional optical path. Instead, as a probe pulse we have used a later pulse from the mode-locked laser which has been given a further small delay by means of a short adjustable optical path. For example, to achieve a delay of 300 ns, we use the 22nd pulse (delayed by 291.5 ns) with an extra path delay of 8.5 ns.

As representative data, Fig. 3 shows the change in reflectivity  $\Delta R(t)$  arising from an acoustic echo in a [110] Ge sample of thickness 0.99 mm. The oscillations in the tail of the pulse are the features due to the dispersion as described above. The open squares are the experimental data points and the solid line is a fit to the data (see description below). The data shown in Fig. 3 were taken at a temperature of 25 K. At higher temperatures the amplitude of the echo decreases. We assume that this is because of the attenuation arising from the anharmonic interactions with thermal phonons. The echo also shifts to later times as the temperature is raised due to a decrease in the sound velocity. To obtain the data shown in Fig. 3 light pulses of energy 0.2 nJ were used to generate the acoustic pulses. A small variation in the pulse energy changes the amplitude of the echo, but does not change the echo shape. But when the pulse energy is increased above about 0.4 nJ, there is

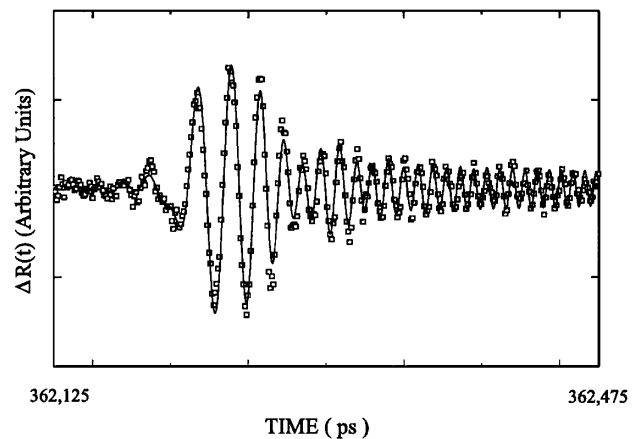


FIG. 3. Picosecond ultrasonic data (open squares) for a longitudinal acoustic pulse propagating in the [110] direction in Ge at 25 K. The oscillations in the tail of the pulse are due to phonon dispersion. The solid curve is a simulation as described in the text.

TABLE I. A summary of the results obtained for the dispersion of silicon and germanium. The thickness of the sample is  $d$ , the sound velocity is  $c$ , and  $\gamma$  is the dispersion parameter defined in Eq. (2). The results for  $\gamma$  are compared with  $\gamma$  obtained from a model with nearest-neighbor forces due to Hsieh (Ref. [14]), from a model by Tamura with interactions out to eighth-nearest neighbors (Ref. [5]), and the adiabatic bond charge model of Weber (Ref. [19]).

Sample	$d$ (mm)	$c$ ( $10^5$ cm/s)	$\gamma_{\text{Exp}}$ ( $10^{-11}$ cm $^3$ s $^{-1}$ )	$\gamma_{\text{Hsieh}}$ ( $10^{-11}$ cm $^3$ s $^{-1}$ )	$\gamma_{\text{Tamura}}$ ( $10^{-11}$ cm $^3$ s $^{-1}$ )	$\gamma_{\text{Weber}}$ ( $10^{-11}$ cm $^3$ s $^{-1}$ )
Si [100]	2.00	8.48	1.80	0.65	1.07	2.20
Si [110]	5.04	9.18	8.45	1.61	6.55	8.00
Si [111]	5.00	9.40	2.55	1.09	3.42	3.52
Ge [100]	0.99	4.97	0.85	0.41	0.85	1.50
Ge [110]	0.99	5.46	5.55	1.01	4.63	5.52
Ge [111]	1.04	5.62	1.05	0.68	2.13	2.46

a significant change in the echo shape [10]. This is presumed to be a result of nonlinear elastic effects. In the experiments reported here, we have used pulse energies small enough that the nonlinear effects are negligible.

To determine the dispersion parameter from the data simulations of the echo shape were performed. These simulations involved a calculation of the shape of the acoustic pulse generated by the Al film, a determination of the change in the shape of this pulse after making a round trip through the sample that results from the dispersion, and calculation of the change in optical reflectivity  $\Delta R(t)$  that takes place when the acoustic pulse reenters the Al film. The simulation for the generation and detection of the acoustic pulses is based on the theory given by Thomsen *et al.* [6]. To include the dispersion and attenuation [11] of the phonons, we have calculated the change of the pulse shape by taking the Fourier transform of the generated pulse, modifying it with a frequency-dependent amplitude and phase, and then transforming it back to the time domain. The simulations use the known density and sound velocity of Al, Ge, and Si [12]. The adjustable parameters are the dispersion  $\gamma$ , the thickness  $d_{\text{Al}}$  of the Al film, the thickness  $d$  of the sample [13], the attenuation  $\alpha$  in the sample, and the optical constants of the Al film (i.e., the dielectric constant and piezo-optic coefficients). Of these adjustable parameters, only  $\gamma$  has a significant effect on the frequency of the oscillations after the arrival of the main echo. Adjustment of the other parameters is important in order to obtain a good fit to the front of the pulse and to the rate at which the oscillations after the pulse decrease in amplitude.

Table I gives the results that we have obtained for the dispersion parameter  $\gamma$ . The uncertainty in these values of  $\gamma$  is typically  $\pm 5\%$ . For both Si and Ge, the largest  $\gamma$  value is found for the [110] direction and the smallest for the [100]. We list in Table I values of  $\gamma$  that we have calculated using different models of lattice dynamics of Si and Ge taken from the literature. We first make a comparison with the model of Hsieh [14]. In this model the interactions are restricted to the nearest neighbors. The model gives  $\gamma$  values that are all significantly less than what we have measured. In addition, the model gives  $\gamma$  values that

vary with direction much less than is found experimentally. For example, in Ge the experiment gives  $\gamma_{110}/\gamma_{100} = 6.5$ , whereas the Hsieh model gives 2.5 for this ratio. A more elaborate model has been constructed by Tamura [5]. This model uses 31 force constants that describe interactions out to eighth-nearest neighbors. The model gives an excellent fit to the dispersion curves as measured by neutron scattering [15–18]. The agreement with the experimental  $\gamma$  is generally much better than for the Hsieh model, presumably because of the inclusion of longer range interactions. However, the degree of agreement varies markedly with direction and from Si to Ge, with no obvious pattern. The third model is the adiabatic bond-charge model due to Weber [19]. This provides the best agreement with the experimental values, but substantially overestimates the dispersion in the [100] and [111] directions for both Si and Ge. Models such as the bond-charge model were originally introduced to explain the anomalous flattening of the transverse acoustic branches at large wave vectors. It will be interesting to consider how such models need to be modified so as to give the correct dispersion for long wavelength acoustic phonons, while still giving the dispersion of the short wavelength transverse phonons correctly.

In summary, we have described how the picosecond ultrasonics technique can be used to measure the dispersion of longitudinal acoustic phonons of long wavelengths. These measurements provide a new test of lattice dynamical models.

We thank C. Elbaum and R. O. Pohl for providing some of the Ge and Si single crystals. This work was supported in part by the U.S. Department of Energy through Grant No. DE-FG03-ER45267.

- 
- [1] N. W. Ashcroft and N. D. Mermin, *Solid State Physics* (Saunders College, Philadelphia, 1976).
  - [2] H. Bilz and W. Kress, in *Phonon Dispersion Relations in Insulators*, edited by M. Cardona and P. Fulde (Springer, New York, 1979).
  - [3] M. P. Kemoklidze and L. P. Pitaevskii, *Sov. Phys. JETP* **32**, 1183 (1971).

- [4] W. Dietsche, G. A. Northrop, and J.P. Wolfe, Phys. Rev. Lett. **47**, 660 (1981).
- [5] Shin-ichiro Tamura, Phys. Rev. B **28**, 897 (1983).
- [6] C. Thomsen, H. T. Grahn, H. J. Maris, and J. Tauc, Phys. Rev. B **34**, 4129 (1986).
- [7] J. Baden-Powell, *View of the Undulatory Theory as Applied to the Dispersion of Light* (J. W. Parker, London, 1841).
- [8] Sir W. R. Hamilton, *Mathematical Papers* (Cambridge University Press, London and New York, 1940).
- [9] A. Maradudin, E. W. Montroll, G. H. Weiss, and I. P. Ipatova, *The Theory of Lattice Dynamics in the Harmonic Approximation* (Academic Press, New York and London, 1971).
- [10] Hsin-Yi Hao and Humphrey J. Maris, Physica (Amsterdam) **263–264B**, 670 (1999).
- [11] The attenuation at low temperature ( $T \leq 40$  K) was taken to vary as  $\alpha_0 \omega^2$ , where  $\alpha_0$  is constant independent of temperature. Inclusion of a frequency-dependent attenuation in the simulation is necessary to cause the oscillations in the tail to damp out at the rate found in the experiment. We find that a quadratic dependency gives a good fit to the experimental data (see Fig. 3). It is possible that this apparent attenuation does not occur in the bulk of the sample, but instead arises from the roughness of the sample surfaces. We have not yet found the theory to fully describe the phonon attenuation at this frequency and temperature range.
- [12] H. J. McSkimin, J. Appl. Phys. **24**, 988 (1953).
- [13] The thickness must be treated as an adjustable parameter because it cannot be measured with sufficient accuracy by conventional means.
- [14] Y-C. Hsieh, J. Chem. Phys. **22**, 306 (1954).
- [15] G. Dolling, *Inelastic Scattering of Neutrons in Solids and Liquids* (IAEA, Vienna, 1963), Vol. I, p. 37.
- [16] G. Nilsson and G. Nelin, Phys. Rev. B **3**, 364 (1971).
- [17] G. Nelin and G. Nilsson, Phys. Rev. B **5**, 3151 (1972).
- [18] G. Nilsson and G. Nelin, Phys. Rev. B **6**, 3777 (1972).
- [19] W. Weber, Phys. Rev. B **15**, 4789 (1977).